On the complex behavior of strain relaxation in (In,Ga)As/GaAs(001) quantum dot molecules

M. Hanke,[1,a)] M. Dubslaff,[1] M. Schmidbauer,[2] Zh. M. Wang,[3] Yu. I. Mazur,[3] P. M. Lytvyn,[3,b)] J. H. Lee,[4] and G. J. Salamo[3]
[1]*Paul-Drude-Institut für Festkörperelektronik, Hausvogteiplatz 5-7, D-10117 Berlin, Germany*
[2]*Leibniz-Institut für Kristallzüchtung, Max-Born-Straße 2, D-12489 Berlin, Germany*
[3]*Department of Physics, University of Arkansas, Fayetteville, Arkansas 72701, USA*
[4]*Department of Electrical Engineering, Kwangwoon University, Seoul 139-701, Republic of Korea*

(Received 14 May 2009; accepted 20 June 2009; published online 13 July 2009)

A detailed growth scenario of surface quantum dot molecules (QDM) in the system (In,Ga)As/GaAs(001) has been investigated in terms of shape and elastic strain evolution. QDMs are grown by a combined approach using droplet epitaxy for initial homoepitaxial GaAs mounds, which subsequently serve as nucleation spots for surrounding (In,Ga)As surface quantum dots. Atomic force micrographs trace a detailed pathway toward the final QDM containing up to six quantum dots with perfect inherent symmetry. Synchrotron-based grazing incidence diffraction together with grazing incidence small angle x-ray scattering reveal a relaxation behavior, which for all growth stages comprises a strained lattice along $[\bar{1}10]$ and partial elastic relaxation along [110]. Numerical finite element calculations on the three-dimensional strain profile support the experimental findings. © *2009 American Institute of Physics*. [DOI: 10.1063/1.3176409]

A widely recognized development in the self-assembly of semiconductor nanostructures is the growth of quantum dot molecules (QDMs). These are local arrangements of a small number (in many cases 2–8) of individual quantum dots (QDs). Besides the most simple kind of prototypical QDM containing just two QDs,[1] more sophisticated QDMs made of three, four, or even six QDs are frequently discussed.[2,3] All the different types (bi-QDMs and multi-QDMs) can be considered as building blocks of different functionality for optoelectronic device applications,[4] future quantum computational devices,[5] and quantum communication.[6] In that context a detailed knowledge on elastic strain evolution (with respect to the particular shape) becomes a key issue for a better understanding of the QDM's evolution.

In this letter we will focus on surface QDMs grown by molecular beam epitaxy on semi-insulating GaAs(001) substrates. Initially, 3 ML of Ga were deposited at the surface temperature of 500 °C on a 0.5 μm GaAs buffer layer. This initially forms metallic Ga droplets on the surface. Subsequently, these droplets were converted into semiconductor nanocrystals with incoming As flux. This process occurs because GaAs is the preferred form when the liquid Ga droplets are exposed to As flux. As a result, they were crystallized into GaAs by the incorporation of As atoms, and thus strain-free, homoepitaxial GaAs mounds[7] with a pronounced asymmetry along the different ⟨110⟩ directions (not shown) can be established. This initial shape asymmetry, which drives the later shape asymmetry of the QMDs, can be attributed to different surface diffusion lengths on GaAs(001).[8] The crystallization was performed at 150 °C to keep the original shape of the droplets. Otherwise, the resulting configurations can be either ring- or lenslike,[9] or even droplets can diffuse away depending on crystallization temperatures.[10] Subsequently, various amounts of InAs were deposited on the GaAs mound template, for this study, namely, 1.6, 1.9, and finally 2.0 ML of InAs—all at a constant surface temperature of 530 °C. Corresponding atomic force micrographs (AFMs), Figs. 1, 2, and 3(a), depict an increasing number of self-assembled (In,Ga)As QDs surrounding the initial GaAs mounds. Due to the additional degree of freedom to relax at those sites they provide favorable energetical conditions for further (heteroepitaxial) (In,Ga)As growth.

Synchrotron-based grazing incidence diffraction (GID) and grazing incidence small angle x-ray scattering

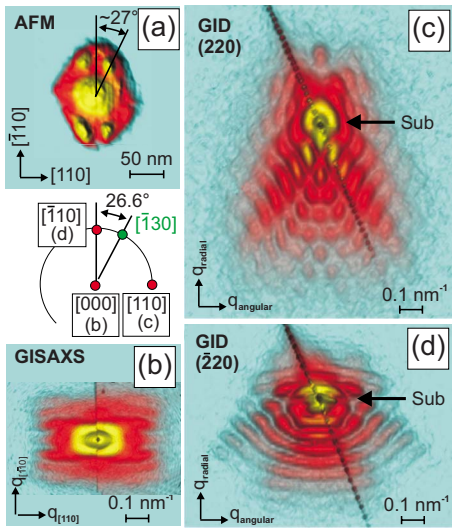

FIG. 1. (Color online) AFM (a) of a single quadruplet-QDM, corresponding to 1.6. ML InAs, and (b) the in-plane GISAXS, which is comparable to the FFT. (c) and (d) give the diffusely scattered intensity near the in-plane (220) and $(\bar{2}20)$ reflections, denoted (Sub). Due to the finite angular acceptance of the analyzer crystal all depicted GID patterns are intersected by a so-called analyzer streak. The stereographic projection shows that the four equivalent corner (In,Ga)As QDs nucleate along the ⟨130⟩ directions. Additionally the reciprocal lattice points probed by GID and GISAXS are highlighted.

a)Electronic mail: hanke@pdi-berlin.de.
b)Present address: V. Lashkaryov Institute of Semiconductor Physics, NAS of Ukraine, Kiev 03028, Ukraine.

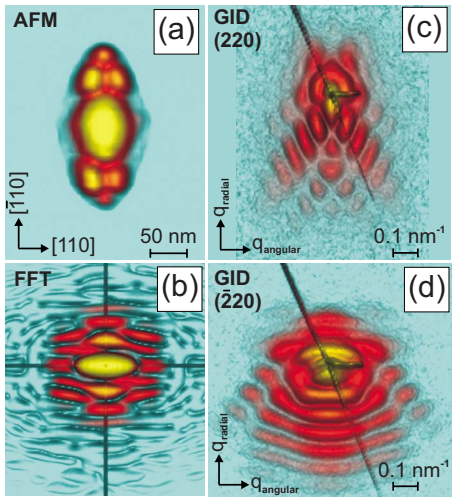

FIG. 2. (Color online) AFM (a) of a intermediated QDM stage, corresponding to 1.9. ML InAs, and its FFT (b). (c) and (d) give the diffusely scattered intensity near the in-plane (220) and ($\bar{2}20$) reflections.

(GISAXS) may provide highly surface sensitive information on low-dimensional semiconductor nanostructures, since the angle of incidence is very small (0.3°), and the incoming x-ray wave field thus decreases exponentially inside the sample. Both the QDM's morphology and the three-dimensional chemical composition profile will mainly drive the established elastic strain and hence change the GID pattern accordingly. Generally a height-dependent gradient of the in-plane lattice constant will contribute to diffusely scattered intensity at different q_{radial} positions (iso-strain scattering,[11]). Thereby intensity at small q_{radial} originates from regions close to the QD apex, while larger values of q_{radial} are due to areas closer to the substrate.

GID and GISAXS measurements were performed at beamline ID10B at the European Synchrotron Radiation Facility (ESRF), Grenoble using an x-ray energy of 8 keV. A

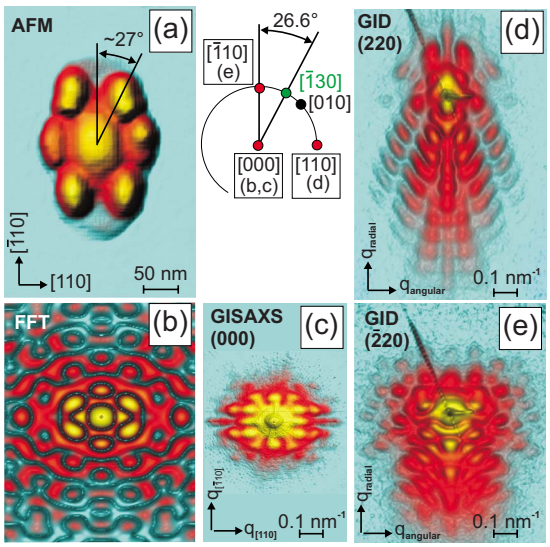

FIG. 3. (Color online) AFM (a) of a single hexa-QDM, corresponding to 2.0 ML InAs, and its FFT (b), which is comparable with the in-plane intensity around the reciprocal origin (c). (d) and (e) give the diffusely scattered intensity near the in-plane (220) and ($\bar{2}20$) reflections. The stereographic projection shows that the four equivalent corner (In,Ga)As QDs nucleate along the ⟨130⟩ directions, as initially in Fig. 1(a). Areas for GID and GISAXS are highlighted as well.

positional sensitive VANTEC detector has been placed about 500 mm behind the sample enabling an angular resolution along different exit angles α_f. Further on an additional crystal analyzer Ge(111) was used to enhance the angular resolution parallel the sample surface to about 0.03 nm^{-1}. Following the evolution from initial QDMs consisting of four QDs, Fig. 1(a), via an intermediate stage, Fig. 2(a), toward hexapodlike structures, Fig. 3(a), the shape and elastic strain asymmetry with respect to the different ⟨110⟩ directions become clearly visible at the diffusely scattered x-ray intensity near the in-equivalent GID(220) and GID($\bar{2}20$) reflections in Figs. 1–3.

From the first view the reader might argue that this asymmetry is primarily and exclusively given by the obvious shape asymmetry, which is not the case. When choosing the in-plane diffraction vector along the [$\bar{1}$10] direction (hence along the longer QDM axis) the GID pattern appears similar to both: the fast Fourier transform (FFT) of the AFMs [Figs. 2(b) and 3(b)], and, alternatively, the GISAXS patterns [Figs. 1(b) and 3(c)], which are also exclusively sensitive to shape. This indicates a rather strained lattice along the [$\bar{1}$10] direction throughout the QDMs. By contrast to that, if the diffraction vector runs along the [110] direction (the shorter QDM axis), the diffraction patterns [Figs. 1(c), 2(c), and 3(d)] reflect a more pronounced elastic relaxation. This behavior can be attributed to the fact that along the smaller lateral extensions, parallel [110], there is less material agglomerated in the QDM, which otherwise may prevent relaxation.

It is well confirmed that individual QDs progressively relax toward their apex, which is not surprising since the substrate impact becomes weaker, e.g., Ref. 12. However, for QDMs the situation becomes more complex due to additional pathways to form their inner symmetry. In our study the accumulated strain (by adding InAs to the GaAs QD template) is preferably relieved by extending the QDM elongation in [$\bar{1}$10] direction. This route is presumably related to different in-plane diffusion lengths as known for the evolution of single InAs QDs on GaAs.[13] It is interesting to note that only in the final growth stage [by deposition of 2.0 ML InAs, Fig. 3(a)] two QDs along [110] appear.

As described before the x-ray scattering gives a clear experimental proof for an anisotropic elastic relaxation. However, it does not provide a picture of its three-dimensional nature. Even more in a partially noncoherent scattering experiment the phase information of the x-ray wavefield gets lost, which means that it is generally impossible to extract the three-dimensional strain profile without making assumptions. In order to calculate the strain field near a QDM we have applied finite element method (FEM): a numerical approach on the base of linear elasticity theory. FEM enables (comparing with other, in particular analytical attempts) the study of a great variety of different shapes and chemical compositions. Within the corresponding FE model of a hexapodlike QDM, as shown in Figs. 4(a) and 4(b), we have considered three different types of QDs: a central GaAs QD (type 1) and two differently rotated (In,Ga)As QDs (type 2 and 3). Figures 4(c) and 4(d) give the two in-plane components of the elastic strain relaxation. Due to particular inner symmetry one can prove a somewhat unexpected strain-modulation along both ⟨110⟩ directions, changing twice its sign: from a laterally expanded (+) lattice [$\Delta y > 0$, green-

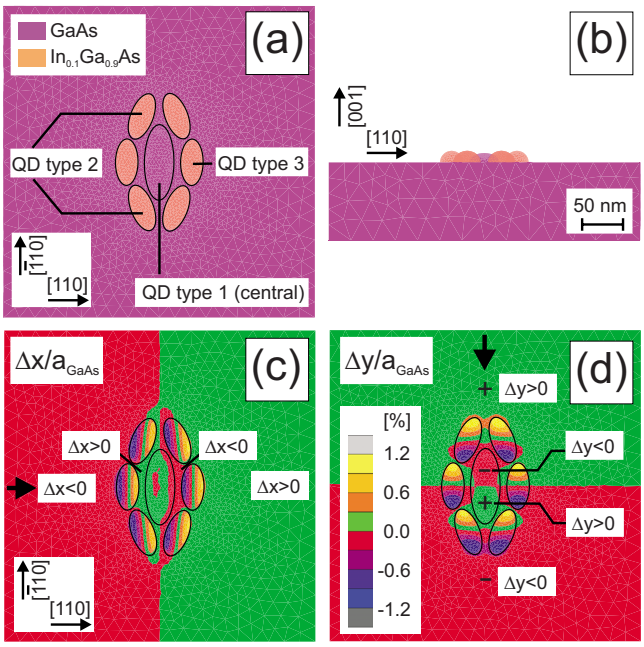

FIG. 4. (Color online) The FE grid (a) and (b) contains on a GaAs(001) substrate the central, nominally strain-free GaAs QD (type 1), the azimuthally tilted InGaAs QDs (type 2), and finally the two InGaAs QDs in [110] and $[\bar{1}\bar{1}0]$ directions (type 3). (c) and (d) show the resulting strain components along [110] and $[\bar{1}10]$. Following the arrows in (c) and (d) the sign of lattice distortion (Δx and Δy) within the substrate changes twice due to the surrounding (In,Ga)As QDs.

colored area outside the QDM in Fig. 4(d)] via an alternatively compressed (−) and expanded (+) lattice underneath the central GaAs QD changing finally again into a compressed lattice. A similar behavior of the orthogonal component Δx is shown for the other direction in Fig. 4(c). This particular (sign-changing) strain modulation is exclusively related to the surrounding (In,Ga)As QDs, while a single heteroepitaxial QD will not cause such a complex strain profile in its vicinity.

In summary, we have probed the evolution of shape and elastic strain during the formation of (In,Ga)As on GaAs(001) QDMs. Subsequent stages show an orientation dependent strain relaxation along the different ⟨110⟩ directions. A combination of x-ray scattering techniques (GID and GISAXS) prove within the QDM a strained lattice along the $[\bar{1}10]$ direction, whereas relaxed unit cells along [110]. This can be attributed to the different elongations of the QDM. Further on FE calculations predict a complex behavior of the in-plane lattice parameter at the QDM-substrate interface, which is directly related to the particular QDM symmetry.

We acknowledge financial support by the German Research Foundation, Project No. HA3495/6-1, the National Science Foundation of the U.S. through Grant No. DMR-0520550 and the European Synchrotron Radiation Facility ESRF in Grenoble for providing beamtime during experiment SI-1870.

[1] M. F. Doty, J. I. Climente, M. Korkusinski, M. Scheibner, A. S. Bracker, P. Hawrylak, and D. Gammon, Phys. Rev. Lett. **102**, 047401 (2009).
[2] H. Yang, X. Zhang, Z. Jiang, X. Yang, and Y. Fan, J. Appl. Phys. **104**, 044303 (2008).
[3] J. H. Lee, K. Sablon, Z. M. Wang, and G. J. Salamo, J. Appl. Phys. **103**, 054301 (2008).
[4] D. Stepanenko and G. Burkard, Phys. Rev. B **75**, 085324 (2007).
[5] H. J. Krenner, M. Sabathil, E. C. Clark, A. Kress, D. Schuh, M. Bichler, G. Abstreiter, and J. J. Finley, Phys. Rev. Lett. **94**, 057402 (2005).
[6] T. Unold, K. Mueller, C. Lienau, T. Elsaesser, and A. D. Wieck, Phys. Rev. Lett. **94**, 137404 (2005).
[7] J. H. Lee, Zh. M. Wang, N. W. Storm, Yu. I. Mazur, and G. J. Salamo, Appl. Phys. Lett. **89**, 202101 (2006).
[8] C. Heyn, A. Stemmann, A. Schramm, and W. Hansen, J. Cryst. Growth **311**, 1825 (2009).
[9] M. Hanke, Yu. I. Mazur, E. Marega, Z. Y. AbuWaar, G. J. Salamo, P. Schäfer, and M. Schmidbauer, Appl. Phys. Lett. **91**, 043103 (2007).
[10] B. L. Liang, Zh. M. Wang, J. H. Lee, K. Sablon, Yu. I. Mazur, and G. J. Salamo, Appl. Phys. Lett. **89**, 043113 (2006).
[11] I. Kegel, T. H. Metzger, A. Lorke, J. Peisl, J. Stangl, G. Bauer, J. M. Garcia, and P. M. Petroff, Phys. Rev. Lett. **85**, 1694 (2000).
[12] I. Kegel, T. H. Metzger, A. Lorke, J. Peisl, J. Stangl, G. Bauer, K. Nordlund, W. V. Schoenfeld, and P. M. Petroff, Phys. Rev. B **63**, 035318 (2001).
[13] M. Schmidbauer, Zh. M. Wang, Yu. I. Mazur, P. M. Lytvyn, G. J. Salamo, D. Girgoriev, P. Schäfer, R. Köhler, and M. Hanke, Appl. Phys. Lett. **91**, 093110 (2007).